

ChemComm

Accepted Manuscript



This is an *Accepted Manuscript*, which has been through the Royal Society of Chemistry peer review process and has been accepted for publication.

Accepted Manuscripts are published online shortly after acceptance, before technical editing, formatting and proof reading. Using this free service, authors can make their results available to the community, in citable form, before we publish the edited article. We will replace this *Accepted Manuscript* with the edited and formatted *Advance Article* as soon as it is available.

You can find more information about *Accepted Manuscripts* in the [Information for Authors](#).

Please note that technical editing may introduce minor changes to the text and/or graphics, which may alter content. The journal's standard [Terms & Conditions](#) and the [Ethical guidelines](#) still apply. In no event shall the Royal Society of Chemistry be held responsible for any errors or omissions in this *Accepted Manuscript* or any consequences arising from the use of any information it contains.

COMMUNICATION

Self-assembly of NH_2 - $(\alpha,\text{L-lysine})_n$ -COOH and SDS into nanodiscs or nanoribbons regulated by pH

Cite this: DOI: 10.1039/x0xx00000x

S. Zhang[†], S. Yang[†], J. Zang[†], R. Yang[†], G. Zhao^{†,*}, and C. Xu^{†,*}

Received 00th January 2014,

Accepted 00th January 2014

DOI: 10.1039/x0xx00000x

www.rsc.org/chemcomm

NH_2 - $(\alpha,\text{L-lysine})_n$ -COOH and SDS can self-assemble into nanodiscs or nanoribbons. We show that pH can regulate not only the diameter of nanodiscs but also the conversion between nanodiscs and nanoribbons. This system can be used as two different templates for fabricating platinum nanowires and nanodiscs.

Molecular self-assembly recently has attracted considerable attention from researchers in the field of nanoscience and nanotechnology.¹⁻⁴ There has been an abundance of research over the past few decades on the design and fabrication of novel biomimetic nanobiomaterials through peptide self-assembly. Many synthetic peptides have recently been explored as useful nanobiomaterials.^{5,6} The structural feature common to most synthetic polypeptide materials is an amphiphilic block copolymer sequence, where either one or more polymer domains is peptidic.^{2,7,8}

Generally, these synthetic polypeptide materials self-assemble into one-dimensional (1D) nanostructures. Interesting examples include the self-assembly of cylindrical micelles,⁹ ribbons,¹⁰ nanofibers,¹¹ and nanobelts.¹² The key factor in formation of these 1D nanostructures is the control of preferential growth in only one dimension. However, two dimensional (2D) peptide materials are rare because of the difficulty of maintaining two similar or identical growth rates along two different dimensions.

Herein, we report a successful case of nanodiscs preparation by self-assembly of a short, linear peptide NH_2 - $(\alpha,\text{L-lysine})_n$ -COOH and anionic surfactant SDS in buffer-free aqueous solution. The formed nanodiscs are very different from the very common one dimensional morphology, such as peptide amphiphiles.^{1,2} The kinetics of the formation of the nanodiscs showed that nanobelts were formed at early stages, and later they converted into concentric nanorings. Interestingly, we found that at $\text{pH} \leq 7.0$, these two small molecules self-assemble into nanodiscs, while only nanoribbons were produced under the same experimental conditions except that

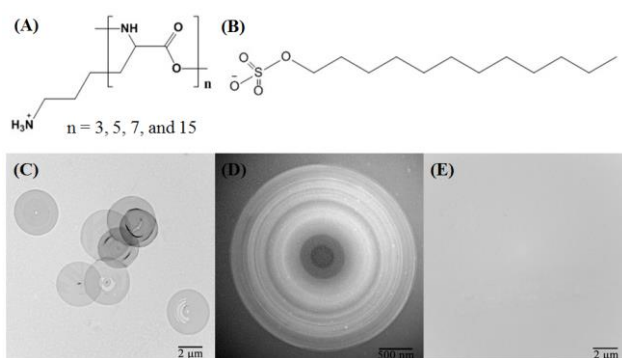


Fig. 1 (A, B) Chemical structure of NH_2 - $(\alpha,\text{L-lysine})_n$ -COOH and SDS. (C, D) TEM images of nanodiscs assembled from NH_2 - $(\alpha,\text{L-lysine})_n$ -COOH and SDS. (E) TEM image showing no nanodiscs upon mixing NH_2 - $(\alpha,\text{L-lysine})_n$ -COOH ($n = 3, 7, \text{ and } 15$) with SDS, respectively.

pH was increased to 11.0. Most excitedly, these two different types of nanostructures can be converted with each other as regulated by pH. We also demonstrate that these pH-sensitive templates can be employed to generate platinum nanodiscs or nanowires.

We carried out original studies on the interaction between NH_2 - $(\alpha,\text{L-lysine})_n$ -COOH ($n = 3, 5, 7, \text{ and } 15$) (Fig. 1A) and SDS (Fig. 1B), respectively. Upon mixing of NH_2 - $(\alpha,\text{L-lysine})_n$ -COOH with SDS molecules (NH_2 - $(\alpha,\text{L-lysine})_n$ -COOH/SDS = $1/2n$) in water, followed by maintaining at room temperature for 3 days, the supernatants were collected from a series of mixtures, respectively. When NH_2 - $(\alpha,\text{L-lysine})_5$ -COOH was used, excitingly, we note the flat, disc-like morphology of the structures formed in aqueous solution. The nanodiscs have fairly monodisperse diameters on the order of 3-4 μm (Fig. 1C). More interestingly, these disc-like structures are composed of a number of concentric nanorings which arrange side by side (Fig. 1D). In contrast, when the polymerization degree of poly($\alpha,\text{L-lysine}$) is either less than 5 ($n = 3$) or higher than 5 ($n = 7 \text{ and } 15$), no such disc-like structure was observed under the same experimental conditions (Fig. 1E). Thus, the length of NH_2 - $(\alpha,\text{L-lysine})_n$ -COOH is pre-requisite for the generation of the nanodiscs.

[†]College of Food Science & Nutritional Engineering, China Agricultural University, Beijing Key Laboratory of Functional Food from Plant Resources, Beijing, 100083, China. E-mail: gzhao@cau.edu.cn; [‡]School of Chinese Medicine (SCM), Chinese University of Hong Kong, Hong Kong, China. E-mail: csxu@cuhk.edu.hk

[†]Electronic Supplementary Information (ESI) available. Experimental details. See DOI: 10.1039/c000000x/

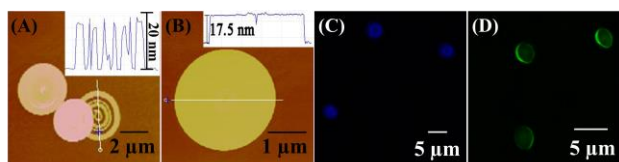


Fig. 2 (A, B) AFM images of nanodiscs. (C, D) LSCM images of nanodiscs upon fluorescence labeling with DAPI and FITC, respectively.

To further characterize such assemblies, atomic force microscope (AFM) in a tapping-mode was used to examine images of the mixture of NH_2 - $(\alpha,\text{L-lysine})_5$ -COOH and SDS at a ratio of 1 to 10 on a freshly cleaved mica surface. The AFM image in Fig. 2A and B shows typical nanostructures of the mixture under the same experimental conditions as TEM. Similarly, well regular nanodiscs were observed, which are composed of concentric nanorings. AFM reveals a small variation in height (between 15 and 20 nm) among the nanodiscs. Since water evaporation involved in TEM and AFM may cause the NH_2 - $(\alpha,\text{L-lysine})_5$ -COOH and SDS to aggregate and alter their morphology, laser scanning confocal microscopy (LSCM) was employed to confirm the assembly of NH_2 - $(\alpha,\text{L-lysine})_5$ -COOH and SDS in solution upon fluorescence labeling with cationic dye DAPI (Fig. 2C) and anionic dye FITC (Fig. 2D) dyes, respectively. Fig. 2C and D show that the nanodisc morphology is indeed the dominant structure in solution. All these results demonstrate that the structure of nanodiscs presented here is completely different from previously reported disc-like micelles.¹³⁻¹⁵

To explore which factor has an effect on the formation of disc-like assemblies, SDS was incubated with NH_2 - $(\alpha,\text{L-lysine})_5$ -COOH (0.4 mM) for 10 h at different ratios in water, respectively, followed by TEM analyses. At the NH_2 - $(\alpha,\text{L-lysine})_5$ -COOH/SDS ratio of 1/6, cylindrical nanostructures were observed (Fig. S1A, Supporting Information), which exhibit lengths well over a few micrometers (up to 10 μm) and widths in the order of 100 nm. Nearly the same results were obtained at the NH_2 - $(\alpha,\text{L-lysine})_5$ -COOH/SDS ratio of 1/2 or 1/4 (data not shown). With decreasing this ratio to 1/10, as expected, concentric nanorings and nanodiscs were revealed by TEM (Fig. S1B). At the ratio of 1/14, irregular nanofibers occurred, which were characterized by several micrometers in length and 10-100 nm in width (Fig. S1C). Thus, the ratio of NH_2 - $(\alpha,\text{L-lysine})_5$ -COOH to SDS appears to be another key factor to regulate the formation of the nanodiscs. When decreasing the concentration of NH_2 - $(\alpha,\text{L-lysine})_5$ -COOH from 0.4 to 0.2 or 0.1 mM at a fixed ratio of NH_2 - $(\alpha,\text{L-lysine})_5$ -COOH/SDS as 1/10, nearly the same but less nanodiscs can be also observed (Fig. S2, Supporting Information), further confirming the above conclusion.

Since pH has been reported to be closely associated with the morphology of nanostructures formed by peptides and their derivatives,¹² effect of pH on the above observed disc-like nanostructures was also investigated. After SDS (4.0 mM) in H_2O was mixed with NH_2 - $(\alpha,\text{L-lysine})_5$ -COOH solution at a NH_2 - $(\alpha,\text{L-lysine})_5$ -COOH/SDS ratio of 1 to 10, the obtained mixture was adjusted to different pH values (5.0, 7.0, and 11.0), respectively, followed by TEM analyses. Cultivation time for all samples was fixed at 3 days. At pH 5.0, interestingly, nanowheel structures were

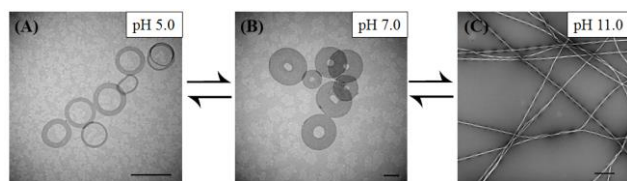


Fig. 3 Effect of pH on both the size of disc-like assemblies and reversible conversion between linear and disc-like assemblies. (A-C) TEM images of assemblies at different pH values. Scale bars represent 500 nm.

formed in aqueous solution, which are multilayered and are composed of a group of concentric rings as revealed by TEM images. The measured outer diameter varies from 350 to 450 nm, and the inner diameter is in the range of 250 to 350 nm (Fig. 3A). In contrast, with increasing pH to 7.0, disc-like morphology of the structures occurs. The size of these disc-like assemblies in outer diameter greatly changes from 400 nm to 2.0 μm , while the inner diameter of these disc-like structures are very similar to each other, which is 200-300 nm in size (Fig. 3B). Thus, pH indeed influences on the size of disc-like nanostructures, which makes it possible that pH acts as a factor to control the size of these nanodiscs. Interestingly, with increasing the pH value to 11.0, no disc-like assembly was observed, and instead these two molecules assembled into ribbons with a twisted morphology (Fig. 3C). These ribbons were 40–60 nm in width, and some of them were tangled together. These results demonstrate that pH is capable of determining the morphology of nanostructures formed by NH_2 - $(\alpha,\text{L-lysine})_5$ -COOH and SDS.

To understand the morphology of NH_2 - $(\alpha,\text{L-lysine})_5$ -COOH and SDS regulated by pH, the critical micelle concentration (cmc) values of SDS in the presence and absence of NH_2 - $(\alpha,\text{L-lysine})_5$ -COOH at pH 5.0 and 11.0 were measured, respectively, as previously described.¹⁶ The cmc of SDS alone was determined to be about 8.0 mM, consistent with a reported value.¹⁶ The cmc of SDS in the presence of NH_2 - $(\alpha,\text{L-lysine})_5$ -COOH at pH 5.0 is slightly decreased to about 7.8 mM most likely because NH_2 - $(\alpha,\text{L-lysine})_5$ -COOH is a small molecule as compared to reported polymers with a much larger molecular weight.^{16,17} In contrast, the cmc of SDS in the presence of NH_2 - $(\alpha,\text{L-lysine})_5$ -COOH at pH 11.0 markedly dropped to 4.0 mM, a value 2-fold lower than that of SDS alone (Fig. S3, Supporting Information). Thus, it is impossible that SDS micelles would present and participate the formation of nanorings and nanodiscs under the present conditions (SDS, 4.0 mM). Agreeing with this idea, no such nanorings and nanodiscs were visualized in the presence of SDS alone with its concentration ranging from 0.5 to 8 mM (not shown). However, it cannot be excluded that SDS micelles might participate the formation of the above mentioned nanoribbons at pH 11.0.

Most excitedly, we found that the morphology of the nanostructures is pH-dependent, and these versatile nanostructures can be converted reversibly with each other. For example, upon changing the solution pH from 5.0 to 7.0, the morphology spontaneously changed from the nanowheels to nanodiscs, and vice versa. Likewise, when increasing the pH value of the same solution from 7.0 to 11.0, the formed nanodiscs were converted into nanoribbons completely as shown in Fig. 3C. Furthermore, after decreasing the solution pH from 11.0 back to 7.0, most of nanoribbons can convert into nanodiscs, suggesting that the 1D nanoribbon can reversibly convert into the 2D disc-like structures.

To obtain mechanistic evidence for the formation of nanodiscs effect of reaction time on nanodisc assemblies was analyzed by TEM. Visually, TEM images illustrate the formation process of disc assemblies from filamentous species to disc assemblies as time continued (Fig. 4A-G). Prior to mixing of NH_2 - $(\alpha,\text{L-lysine})_5$ -COOH with SDS, each of these two molecules were hardly visualized with

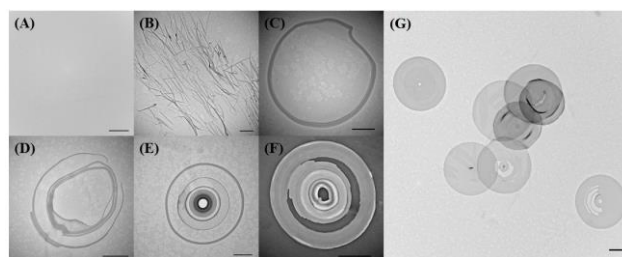


Fig. 4 Kinetics of the formation of nanodiscs revealed by TEM. (A-G) TEM images of assemblies at 0 h, 1 h, 2 h, 5 h, 10 h, 24 h, and 3 days, respectively. Scale bars represent 1.0 μm .

TEM (Fig. 4A). The addition of NH_2 - $(\alpha,\text{L-lysine})_5$ -COOH to SDS initiated the self-assembly reaction. TEM images showed that the early phases of assemblies (1 h) were characterized by belt-like nanostructures. However, nanoring began to appear at the time of 2 h (Fig. 4C). After 5 h, a larger nanoring species was forming along a group smaller and irregular nanorings, indicative of a gradual transition from the nanoring to the concentric nanoring. The above observation suggested that the concentric ring structures were generated from inside to outside (Fig. 4D). At 10 h, one can see well-shaped concentric nanoring structures (Fig. 4E). Fig. 4F showed that a nanodisc is generating by filling the space between these concentric nanorings at 24 h. After 3 days, a family of intact discs were produced, most of which are full of nanorings (Fig. 4G). These results provided the first direct mechanistic evidence for the formation of nanodiscs, namely, nanobelts \rightarrow nanorings \rightarrow concentric nanorings \rightarrow intact nanodiscs.

To shed light on the mechanism of self-assembly morphology of NH_2 - $(\alpha,\text{L-lysine})_5$ -COOH and SDS, the solution chemistry of the assembly reaction was investigated by isothermal titrate calorimetry (ITC). Fig. S4A shows the raw ITC data for a titration of SDS with NH_2 - $(\alpha,\text{L-lysine})_5$ -COOH at pH 7.0. The integrated heats for each injection are shown after subtraction of the control injection in buffer alone. The negative peaks seen in Fig. S4A correspond to an exothermic reaction. The heats for each injection begin to decrease with an increase in the molar ratio of NH_2 - $(\alpha,\text{L-lysine})_5$ -COOH to SDS, and there is little heat change in the end, indicating that the reaction is complete. The ITC data were best fitted to an independent binding model (Fig. S4B), giving an apparent equilibrium constant $K = (7.09 \pm 0.15) \times 10^4 \text{ M}^{-1}$ with the reaction NH_2 - $(\alpha,\text{L-lysine})_5$ -COOH/SDS stoichiometry of 0.22 ± 0.01 , indicating that one NH_2 - $(\alpha,\text{L-lysine})_5$ -COOH binds up to five SDS molecules, producing a new complex. The apparent binding constant is comparable with that of cationic pentapeptides to negatively charged lipid membranes,¹⁸ indicating that NH_2 - $(\alpha,\text{L-lysine})_5$ -COOH binds with SDS through electrostatic interactions, being in good agreement with their structure (Fig. 1A and B). Since the ϵ - NH_2 groups of side chains of NH_2 - $(\alpha,\text{L-lysine})_5$ -COOH are stronger than its α - NH_2 in basicity, it is most likely that five of SDS molecules bind with five side chains of NH_2 - $(\alpha,\text{L-lysine})_5$ -COOH through the electrostatic interaction to form new complexes in solution at pH 7.0 as shown in Fig. S4E. These new complexes are distinct from all reported alkylated peptide amphiphiles in that they have two hydrophilic heads, and five hydrophobic tails. Furthermore, a negative value of $\Delta G^\circ (-27.69 \pm 0.05 \text{ kJ/mol})$ is consistent with the fact that the polymerization reaction of NH_2 - $(\alpha,\text{L-lysine})_5$ -COOH and SDS occurs spontaneously. Similarly, the value of $\Delta S^\circ (-62.69 \pm 4.26 \text{ J/mol}\cdot\text{K})$ is also negative (Table S1), demonstrating that all molecules in the whole system arrange in a more ordered manner upon mixing of NH_2 - $(\alpha,\text{L-lysine})_5$ -COOH with SDS, a typical feature for the polymerization reaction.¹⁷ ΔH° of the reaction is $-46.38 \pm 1.12 \text{ kJ/mol}$ (Table S1), indicative of an exothermic reaction, which is the most key factor to drive NH_2 - $(\alpha,\text{L-lysine})_5$ -COOH and SDS to assemble into the above observed disc-like nanostructures.

To explore the secondary structure of the nanodiscs, we also performed CD studies upon mixing NH_2 - $(\alpha,\text{L-lysine})_5$ -COOH with SDS at a ratio of 1/10 at different pH values. As expected, the 0.4 mM of NH_2 - $(\alpha,\text{L-lysine})_5$ -COOH in water was found to be a random coil secondary structure signaled by the minimum around 198 nm.^{20,21} In contrast, CD spectrum of the mixture at pH 5.0 or 7.0 showed a positive Cotton effect around 195 nm and a negative Cotton effect around 215 nm, indicative of a typical β -sheet conformation (Fig. S5). These results elucidate that the intermolecular H-bond in the peptide regions plays a crucial role in the generation of the disc-like structures. Although the literature suggests that at least six residues are required to form stable β -sheet

structures while the α -helices usually have an average length of ~ 12 residues to stabilize conformations,^{22,23} the short peptide chain of the NH_2 - $(\alpha,\text{L-lysine})_5$ -COOH with only five residues can also form β -sheet in the presence of SDS. In contrast, when adjusting pH to 11.0, a completely different CD spectrum was observed, which is characterized by a large negative peak at $\sim 197 \text{ nm}$, a typical random coil secondary structure. Thus, the conformation of NH_2 - $(\alpha,\text{L-lysine})_5$ -COOH at pH 11.0 is distinctive from that at pH 5.0 or 7.0. Such distinction in the peptide conformation could result in completely different assemblies as observed in Fig. 3.

The disc-like structures were further characterized by small-angle X-ray diffraction (SAXD). The SAXD pattern of the SDS powder is presented for comparison (Fig. S6). The peak corresponding to the lamellar spacing of SDS (39.3 Å) is much sharper than other peaks. From the SAXD spectra, it was observed that there is a small amount of free SDS occurring in the sample. The SAXD pattern of the powder of the mixture of NH_2 - $(\alpha,\text{L-lysine})_5$ -COOH and SDS consists of a new strong peak of high intensity with a Bragg spacing of about 25.3 Å (Fig. S6), indicative a linear structure with a long period spacing of 25.3 Å. The length of the fully extended dodecyl sulfate chain is about 16 Å, and the distance between the α -carbon and the terminal nitrogen atom in NH_2 - $(\alpha,\text{L-lysine})_5$ -COOH is about 6 Å.^{24,25} On the basis of the value of the linear long period of 25.3 Å, we conclude that surfactant chains in the complex are interdigitated as shown in Fig. S7. Thus, in the system of NH_2 - $(\alpha,\text{L-lysine})_5$ -COOH and SDS, newly formed complexes consisting of one NH_2 -molecule of $(\alpha,\text{L-lysine})_5$ -COOH and five SDS molecules by electrostatic interactions (Fig. S4) actually act as building blocks to assemble into the observed disc-like structures.

Platinum nanostructures have been attracting active attention due to many technical applications,²⁶⁻²⁸ including as an electrocatalyst in proton exchange membrane fuel cells and as catalysts in many reactions including solar water-splitting devices.^{29,30} However, how to control the shape of the platinum nanostructures is a challenge. To explore the application of the different NH_2 - $(\alpha,\text{L-lysine})_5$ -COOH/SDS assemblies for the preparation of platinum nanomaterials, firstly, an aged K_2PtCl_4 aqueous solution was incubated with the NH_2 - $(\alpha,\text{L-lysine})_5$ -COOH/SDS disc-like assemblies, followed by treatment with glutaraldehyde used as a crosslinking reagent. After reduction by ascorbic acid, a disc-like 2D array of platinum nanoparticles (PtNPs) was visualized by TEM (Fig. S8A). The magnified image shows a sophisticated 2D superstructure, where the PtNPs were immobilized on both sides of the NH_2 - $(\alpha,\text{L-lysine})_5$ -COOH/SDS discs, which functioned as a template (Fig. S8B and C). In contrast, such platinum disc-like arrangement lacked with either aged K_2PtCl_4 plus ascorbic acid or the nanodiscs plus aged K_2PtCl_4 in the absence of glutaraldehyde (Fig. S8D) at pH 5.0 or 11.0.

Platinum wires were also prepared using NH_2 - $(\alpha,\text{L-lysine})_5$ -COOH/SDS nanoribbons as templates at pH 11.0 under similar conditions except that no glutaraldehyde was used. TEM images reveal the presence of abundant long platinum nanowires in a low magnification image (Fig. S8E). At higher magnification (Fig. S8F), the nanowires are observed to be twisted and have an average cross-sectional diameter of $\sim 150 \text{ nm}$. Thus, one simple system of NH_2 - $(\alpha,\text{L-lysine})_5$ -COOH/SDS can act as two completely different templates as controlled by pH to fabricate both 1D and 2D platinum nanomaterials.

In closing, a novel, simple system consisting of NH_2 - $(\alpha,\text{L-lysine})_5$ -COOH and SDS can trigger self-assembly into nanodiscs or nanoribbons. We found that pH can regulate not only the diameter of nanodiscs, but the conversion between nanoribbons and nanodiscs. This work highlights one important concept that was previously unrecognized; namely, by regulating pH, 1D peptide biomaterials can convert into 2D ones, and vice versa. These biomaterials can be

used as templates to fabricate platinum nanomaterials with shape control.

This work was supported by the National Science and Technology Support Program (2011BAD23B04)

Notes and references

- 1 S. Scanlon, A. Aggeli, *Nanotoday* 2008, **3**, 22–30.
- 2 X. B. Zhao, F. Pan, H. Xu, M. Yaseen, H. H. Shan, C. A. E. Hauser, S. G. Zhang, J. R. Lu, *Chem. Soc. Rev.* 2010, **39**, 3480–3498.
- 3 E. H. C. Bromley, K. Channon, E. Moutevelis, D. N. Woolfson, *ACS Chem. Biol.* 2008, **3**, 38–50.
- 4 G. Schreiber, G. Haran, H.-X. Zhou, *Chem. Rev.* 2009, **109**, 839–860.
- 5 G. W. M. Vandermeulen, H. A. Klok, *Macromol. Biosci.* 2004, **4**, 383–398.
- 6 H. A. Klok, *Chem.Int. Ed.* 2002, **41**, 1509–1513.
- 7 J. D. Hartgerink, E. Beniash, S. I. Stupp, *Science* 2001, **294**, 1684–1688.
- 8 J. D. Hartgerink, E. Beniash, S. I. Stupp, *Proc. Natl. Acad. Sci. U.S.A.* 2002, **99**, 5133–5138.
- 9 H. G. Cui, Z. Y. Chen, S. Zhong, K. L. Wooley, D. J. Pochan, *Science* 2007, **317**, 647–650.
- 10 E. R. Zubarev, E. D. Sone, S. I. Stupp, *Chem.-Eur. J.* 2006, **12**, 7313–7327.
- 11 M. R. Caplan, E. M. Schwartzfarb, S. G. Zhang, R. D. Kamm, D. A. Lauffenburger, *Biomaterials* 2002, **23**, 219–227.
- 12 H. Cui, T. Muraoka, A. G. Cheetham, S. I. Stupp, *Nano Lett.* 2009, **9**, 945–951.
- 13 T. Zemb, M. Dubois, B. Deme, T. Gulik-Krzywicki, *Science* 1999, **283**, 816–819.
- 14 T. A. Waggoner, J. A. Last, P. G. Kotula, D. Y. Sasaki, *J. Am. Chem. Soc.* 2001, **123**, 496–497.
- 15 H. T. Jung, S. Y. Lee, E. W. Kaler, B. Coldren, J. A. Zasadzinski, *Proc. Natl. Acad. Sci. U.S.A.* 2002, **99**, 15318–15322.
- 16 J. K. Tzeng, S. S. Hou *Macromolecules*. 2008, **41**, 1281–1288.
- 17 M. Shannigrahi, S. Bagchi, *J. Phys. Chem. B.* 2005, **109**, 14567–14572
- 18 M. Hoernke, C. Schwieger, A. Kerth, A. Blume, *Biochim. Biophys. Acta* 2012, **1818**, 1663–1672.
- 19 L. A. Rodríguez-Guadarrama, S. K. Talsania, K. K. Mohanty, R. Rajagopalan, *Langmuir* 1999, **15**, 437–446.
- 20 M. L. Deng, D. F. Yu, Y. B. Hou, Y. L. Wang, *J. Phys. Chem. B* 2009, **113**, 8539–8544.
- 21 P. Manavalan, W. C. Johnson, *Nature* 1983, **305**, 831–832.
- 22 J. Y. Su, R. S. Hodges, C. M. Kay, *Biochemistry* 1994, **33**, 15501–15510.
- 23 A. Aggeli, M. Bell, N. Boden, J. N. Keen, T. C. B. McLeish, I. Nyrkova, S. E. Radford, A. Semenov, *J. Mater. Chem.* 1997, **7**, 1135–1145.
- 24 E. A. Ponomarenko, D. A. Tirrell, W. J. MacKnight, *Macromolecules* 1996, **29**, 8751–8758.
- 25 E. A. Ponomarenko, D. A. Tirrell, W. J. MacKnight, *Macromolecules* 1998, **31**, 1584–1589.
- 26 B.D. McNicol, D.A.J. Rand, K.R. Williams, *J. Power Sources.* 1999, **83**, 15–31.
- 27 E. Antolini, *Mater. Chem. Phys.* 2003, **78**, 563–573.
- 28 D. R. Rolison, *Science* 2003, **299**, 1698–1701.
- 29 P. J. Cameron, L. M. Peter, S. M. Zakeeruddin, M. Gratzel, *Coord. Chem. Rev.* 2004, **248**, 1447–1453.
- 30 X. M. Fang, T. L. Ma, G. Q. Guan, M. Akiyama, E. Abe, *J. Photochem. Photobiol.* 2004, **164**, 179–182.